

3 UNVEILING THE NATURE OF THE UNIDENTIFIED GAMMA-RAY SOURCES V:
4 ANALYSIS OF THE RADIO CANDIDATES WITH THE KERNEL DENSITY ESTIMATION

5 F. MASSARO¹, R. D'ABRUSCO², A. PAGGI², N. MASETTI³,
6 M. GIROLETTI⁴, G. TOSTI⁵, HOWARD, A. SMITH², & S. FUNK¹.

version August 21, 2013: fm

7 ABSTRACT

8 Nearly one-third of the γ -ray sources detected by *Fermi* are still unidentified, despite significant
9 recent progress in this effort. On the other hand, all the γ -ray extragalactic sources associated in the
10 second *Fermi*-LAT catalog have a radio counterpart. Motivated by this observational evidence we
11 investigate all the radio sources of the major radio surveys that lie within the positional uncertainty
12 region of the unidentified γ -ray sources (UGSs) at 95% level of confidence. First we search for their
13 infrared counterparts in the all-sky survey performed by the Wide-field Infrared Survey Explorer
14 (*WISE*) and then we analyze their IR colors in comparison with those of the known γ -ray blazars.
15 We propose a new approach, based on a 2-dimensional kernel density estimation (KDE) technique in
16 the single [3.4]-[4.6]-[12] μm *WISE* color-color plot, replacing the constraint imposed in our previous
17 investigations on the detection at $22\mu\text{m}$ of each potential IR counterpart of the UGSs with associated
18 radio emission. The main goal of this analysis is to find distant γ -ray blazar candidates that, being too
19 faint at $22\mu\text{m}$, are not detected by *WISE* and thus are not selected by our purely IR based methods.
20 We find fifty-five UGS's likely correspond to radio sources with blazar-like IR signatures. Additional
21 eleven UGSs having, blazar-like IR colors, have been found within the sample of sources found with
22 deep recent ATCA observations.

23 *Subject headings*: galaxies: active - galaxies: BL Lacertae objects - radiation mechanisms: non-thermal

24 1. INTRODUCTION

25 The large majority of the point sources detected by
26 the Compton Gamma-ray Observatory in the 1990s (e.g.,
27 Hartman et al. 1999) are still lacking an association with
28 a low-energy candidate counterpart, and given their sky
29 distribution, a significant fraction of these unresolved
30 objects are expected to have extragalactic origin (e.g.,
31 Thompson 2008; Abdo et al. 2010a). Unveiling the ori-
32 gin of the unidentified γ -ray sources (UGSs) is also one
33 of the key scientific objectives of the recent *Fermi* mis-
34 sion that still lists about 1/3 of the γ -ray sources as
35 unassociated in the second *Fermi*-LAT catalog (2FGL;
36 Nolan et al. 2012).
37 A large fraction of UGSs is expected to be blazars, the
38 largest known population of γ -ray active galaxies, not yet
39 associated and/or recognized due to the lack of multifre-
40 quency observations (Ackermann et al. 2011a). There-
41 fore a better understanding of the nature of the UGSs
42 is crucial to estimate accurately the blazar contribu-
43 tion to the extragalactic gamma-ray background (e.g.,
44 Mukherjee et al. 1997; Abdo et al. 2010b), and it is es-
45 sential to constrain exotic high-energy physics phenom-
46 ena (e.g., Zechlin et al. 2012).
47 Many attempts have been adopted to decrease UGSs

48 number and to understand their composition. Pointed
49 *Swift* observations
50 (e.g., Mirabal 2009; Mirabal & Halpern 2009;
51 Paggi et al. 2013) to search for X-ray counterparts of
52 UGSs as well as radio follow up observations were already
53 performed or are still in progress (e.g., Kovalev 2009a;
54 Kovalev et al. 2009b; Petrov et al. 2013). In addition,
55 statistical approaches based on different techniques
56 have been also developed and successfully used (e.g.
57 Mirabal & Pardo 2010; Ackermann et al. 2012).
58 We recently addressed the problem of searching γ -
59 ray blazar candidates as counterparts of the UGSs
60 adopting two new approaches: the first is based on
61 the Wide-field Infrared Survey Explorer (*WISE*) all-
62 sky observations (Wright et al. 2010) aiming at rec-
63 ognizing γ -ray blazar candidates using their peculiar
64 IR colors (Massaro et al. 2011a; D'Abrusco et al. 2012;
65 Massaro et al. 2012b; D'Abrusco et al. 2013) while the
66 second employs the low-frequency radio observations
67 (Massaro et al. 2013b). In particular, this second
68 method was indeed based on the combination of the
69 radio observations Westerbork Northern Sky Survey
70 (WENSS; Rengelink et al. 1997) at 325 MHz with those
71 of the NRAO Very Large Array Sky survey (NVSS;
72 Condon et al. 1998) and of the Very Large Array Faint
73 Images of the Radio Sky at Twenty-Centimeters (FIRST;
74 Becker et al. 1995; White et al. 1997) at about 1.4 GHz.
75 It is worth noting that all the *Fermi* extragalactic
76 sources associated in the 2FGL catalog have a clear radio
77 counterpart (Nolan et al. 2012), this is the basis of the
78 radio- γ -ray connection, that has been found in the case of
79 blazars (e.g., Ghirlanda et al. 2010; Mahony et al. 2010;
80 Ackermann et al. 2011b). Thus, motivated by this ob-
81 servational evidence we propose a different approach to
82 search for the blazar-like counterparts of the UGSs. We

¹ SLAC National Laboratory and Kavli Institute for Particle
Astrophysics and Cosmology, 2575 Sand Hill Road, Menlo Park,
CA 94025, USA

² Harvard - Smithsonian Astrophysical Observatory, 60 Gar-
den Street, Cambridge, MA 02138, USA

³ INAF - Istituto di Astrofisica Spaziale e Fisica Cosmica di
Bologna, via Gobetti 101, 40129, Bologna, Italy

⁴ INAF Istituto di Radioastronomia, via Gobetti 101, 40129,
Bologna, Italy

⁵ Dipartimento di Fisica, Università degli Studi di Perugia,
06123 Perugia, Italy

Submitted to *Astrophysical Journal*.

combine the radio and the IR information available for the sources lying within the positional uncertainty regions of the *Fermi* UGSs to select γ -ray blazar candidates.

With respect to our previous IR based search for blazar-like counterparts (e.g., Massaro et al. 2012a; D’Abrusco et al. 2013) our new analysis relaxes the constraint on the $22\mu\text{m}$ detection of the *WISE*-selected candidates, and does not take into account their $[12]$ - $[22]\mu\text{m}$ color, replacing these features with the presence of a radio counterpart. The number of γ -ray blazars undetected at $22\mu\text{m}$ is only a small fraction ($\sim 8\%$ of the total number of γ -ray blazars D’Abrusco et al. 2013), but includes several high redshift sources that lying at larger distance than the whole population.

To perform our analysis, we search all the radio sources detected in the

NVSS (Condon et al. 1998) and in the Sydney University Molonglo Sky Survey (SUMSS; Mauch et al. 2003) surveys that lie within the positional uncertainty region, at 95% level of confidence, of the UGSs listed in the 2FGL. Then we associate them with their *WISE* counterparts to compare their IR colors with those of the known γ -ray blazars in the $[3.4]$ - $[4.6]$ - $[12]\mu\text{m}$ plot using the kernel density estimation (KDE) technique (e.g., Richards et al. 2004; D’Abrusco et al. 2009; Massaro et al. 2012a). We also verified if the radio sources found in the recent deep radio observations performed by Australia Telescope Compact Array (ATCA) and presented by Petrov et al. (2013) have an IR counterpart with *WISE* colors consistent with those of the γ -ray blazar population. Our analysis of the IR colors is restricted only to the $[3.4]$ - $[4.6]$ - $[12]\mu\text{m}$ color-color plot.

The paper is organized as follows: Section 2 is devoted to the definitions of the samples used while in Section 3 we describe the KDE technique used to perform our investigation; we then applied our selection in Section 4 to identify those radio sources that could be considered blazar-like counterpart of the UGSs listed in the 2FGL catalog. We also verified the presence of optical and X-ray counterparts for the selected γ -ray blazar candidates and we compare our results with different approaches previously developed. Finally, Section 5 is dedicated to our conclusions.

For our numerical results, we use cgs units unless stated otherwise. Spectral indices, α , are defined by flux density, $S_\nu \propto \nu^{-\alpha}$ and *WISE* magnitudes at the $[3.4]$, $[4.6]$, $[12]$, $[22]\mu\text{m}$ (i.e., the nominal *WISE* bands) are in the Vega system respectively. All the magnitudes and the IR colors reported in the paper have been corrected for the Galactic extinction according to the formulae reported in Draine (2003) as also performed in our previous analysis (e.g., D’Abrusco et al. 2013; Massaro et al. 2013a). The most frequent acronyms used in the paper are listed in Table 1.

2. SAMPLE SELECTION

The first sample used in our analysis lists all the blazars listed in the Multiwavelength Blazar Catalog⁶ (ROMA-BZCAT, Massaro et al. 2009) that have been associated as counterparts of *Fermi* sources in the 2FGL

TABLE 1
LIST OF MOST FREQUENT ACRONYMS.

Name	Acronym
Multifrequency Catalog of blazars	ROMA-BZCAT
Second <i>Fermi</i> Large Area Telescope Catalog	2FGL
BL Lac object	BZB
Flat Spectrum Radio Quasar	BZQ
Blazar of Uncertain type	BZU
Unidentified Gamma-ray Source	UGS
Training Blazar sample	TB
Northern UGS sample	NU
Southern UGS sample	SU
Southern Deep ATCA sample	SDA
Kernel Density Estimation	KDE

(Nolan et al. 2012) with a *WISE* counterpart detected at least in the first three filters regardless of the fact that they are detected at $22\mu\text{m}$. The association radius between the ROMA-BZCAT catalog and the *WISE* all-sky survey adopted here was fixed to $3''.3$ (see D’Abrusco et al. 2013, for more details). This sample, named *training blazar* (TB) sample, comprises a total of 737 blazars, excluding those classified as blazars of uncertain type (BZUs) (see also Massaro et al. 2010; Massaro et al. 2011b). The TB sample is used to build the isodensity contours for the KDE technique (see following sections) and to test if IR sources with radio counterparts have *WISE* colors consistent with the γ -ray blazar population.

Then the UGSs sample considered is the one constituted by all the *Fermi* sources listed in the 2FGL with no assigned counterpart at low energies and without any γ -ray analysis flag listing 299 sources (Nolan et al. 2012). We further divided this sample in two subsamples: the northern UGS (NU) sample where only sources with Declination above than -40 deg and the southern UGS (SU) sample selecting those at Declination below -30 deg. This subdivision has been chosen on the basis of the footprints of the radio surveys used for our analysis, since the NU sample is mainly covered by the NVSS survey (Condon et al. 1998), while the SU one by the SUMSS catalog (Mauch et al. 2003). The former sample lists 209 UGSs while 115 sources belong to the latter one.

Finally, we also considered the list of all the radio sources recently found by Petrov et al. (2013) using deep ATCA observations for the UGSs in the southern hemisphere. This sample is labeled as southern deep ATCA (SDA) sample.

3. KERNEL DENSITY ESTIMATION

The KDE technique is a non-parametric procedure to estimate the probability density function of a multivariate distribution without requiring any assumption about the shape of the “parent” distribution. The KDE technique also permits to reconstruct the density distribution of a population of points in a general N -dimensional space based on a finite sample. This analysis depends on only one parameter, the bandwidth of the kernel of the density estimator (analogous to the window size for one-dimensional running average) that can be estimated locally (see e.g., Richards et al. 2004; D’Abrusco et al. 2009; Laurino & D’Abrusco 2011, and reference therein).

⁶ <http://www.asdc.asi.it/bzcat/>

We already applied the KDE technique in several cases to compare the IR colors of blazar candidates selected with different procedures with those of the known population of γ -ray blazars (see Massaro et al. 2011a; Massaro et al. 2012a; Paggi et al. 2013, for more details). Thus in the present analysis we use the KDE method to compare the IR colors of the radio selected counterparts with those of the γ -ray blazar population represented by the TB sample in the 2-dimensional [3.4]-[4.6]-[12] μm color-color plot. As already described in Massaro et al. (2012a), we provide an associated confidence π_{kde} drawn from the KDE density probabilities that a selected radio source as IR colors consistent with the blazars in the TB sample.

In Figure 1 we show the density profiles constructed for the whole blazar population (left panel) and used to estimate π_{kde} and those of the two subsamples of BZBs and BZQs (right panel) belonging to the TB sample, to highlight the dichotomy between the two subclasses.

4. UNIDENTIFIED γ -RAY SOURCES

4.1. Selection of γ -ray blazar candidates

For each UGS we searched for all the radio sources that lie within their positional uncertainty regions at 95% level of confidence and we found that there are 822 radio sources potential counterparts of 209 UGSs and 134 out of 115 for the NU and the SU samples, respectively. We then crossmatched all these radio sources with the *WISE* all-sky catalog⁷ (Wright et al. 2010) using the same radius of 3".3 and we selected only those with an IR counterpart detected at least in the first three *WISE* filters and not extended (i.e., extension flag, $ext_flg \leq 1$) (Cutri et al. 2012). The 3".3 radius chosen to associated sources between the *WISE* and the radio catalogs is statistically justified on the basis of the analysis performed over the entire ROMA-BZCAT (see D'Abrusco et al. 2013, for more details). Thus we obtained 374 out of 822 and 78 out of 134 radio sources in the NU and SU samples, respectively.

Subsequently, we applied the KDE technique described in Section 3 to find radio sources with *WISE* counterparts having IR colors consistent with the γ -ray blazar population. We considered reliable γ -ray blazar candidates only radio sources consistent within the isodensity contours, drawn from the KDE, at 90% level of confidence, correspondent to an association confidence (π_{kde}) greater than 10.0.

We found 41 and 14 radio sources *WISE* selected with $\pi_{kde} > 0.1$ within the NU and the SU samples, respectively. In addition, only 11 out of 416 radio sources listed in the SDA sample have an IR counterpart consistent with the *Fermi* blazar population of the TB sample with $\pi_{kde} > 10.0$. We also list two exceptions to the above criteria: the UGS 2FGLJ1223.3+7954 with its *WISE* blazar candidate WISE J122358.17+795327.8 in the NU sample and 2FGLJ0523.3-2530 with WISE J052313.07-253154.4 as potential counterpart in the SDA sample, having the π_{kde} values equal to 9.6 and 9.5, respectively, marginally below our threshold. The total number of γ -ray blazar candidates is 66 all listed in Table 2 and Table 3. It is worth noting that we do not have any multiple γ -

ray blazar candidate within the positional uncertainty regions of the UGSs analyzed.

In Figure 2 we show the isodensity contours derived from the KDE analysis in the [3.4]-[4.6]-[12] μm color plot, together with the γ -ray blazar candidates selected in the UGS samples analyzed and in the SDA list. It is evident how the large fraction for the selected candidates are located within with the isodensity contours drawn for the BZB class.

To establish if the γ -ray blazar candidate selected with our method have additional multifrequency properties that could confirm their nature and provide redshift estimates, we also searched for the counterpart of our radio-IR selected candidates in the following major surveys. For the near-IR we used only the Two Micron All Sky Survey (2MASS; Skrutskie et al. 2006, 200 - M) since each *WISE* source is already associated with the closest 2MASS source by the default catalog (see Cutri et al. 2012, for more details). We then searched for optical counterparts, with possible spectra available, in the Sloan Digital Sky Survey (SDSS; e.g. Adelman-McCarthy et al. 2008; Paris et al. 2012, - s), in the Six-degree-Field Galaxy Redshift Survey (6dFGS; Jones et al. 2004; Jones et al. 2009, - 6), in the The Muenster Red Sky Survey (MRSS; Ungruhe et al. 2003) and in the USNO-B Catalog (Monet et al. 2003) within 3".3. These optical cross correlations are also useful to plan follow up observations thus a complete list of sources together with their optical magnitudes is reported in Table 4. For the high energy we looked in the soft X-rays using the ROSAT all-sky survey catalog (RASS; Voges et al. 1999, - X). Finally, we also considered the NASA Extragalactic Database (NED)⁸ for any possible counterpart within 3".3 for additional information. The results of this multifrequency investigation is presented and summarized in Table 2 and Table 3.

4.2. Probability of spurious associations

We estimated the probability that our γ -ray blazar candidates can be spurious associations adopting the following approach, similar to that successfully used in our previous analyses (e.g., Massaro et al. 2013b; Paggi et al. 2013).

We created two fake γ -ray catalogs shifting the coordinates of the 41 γ -ray blazars in the NU sample and of the 25 in the SU one by $0^\circ.7$ in a random direction of the sky within the footprints of the NVSS and the SUMSS radio surveys. Keeping the same values of θ_{95} of each fake UGS, we verified that there were no correspondences with real *Fermi* sources within a circular region of radius θ_{95} at the flux level of the 2FGL.

For each fake UGSs, we search for all the radio sources lying within the positional uncertainty region at 95% of confidence in both the NVSS and SUMSS radio surveys. We then checked the presence of an IR counterpart of each radio source selected above crossmatching the *WISE* all-sky catalog with their NVSS and SUMSS positions within a radius of 3".3. The value of this IR-to-radio association radius has been chosen on the basis

⁷ <http://wise2.ipac.caltech.edu/docs/release/allsky/>

⁸ <http://ned.ipac.caltech.edu/>

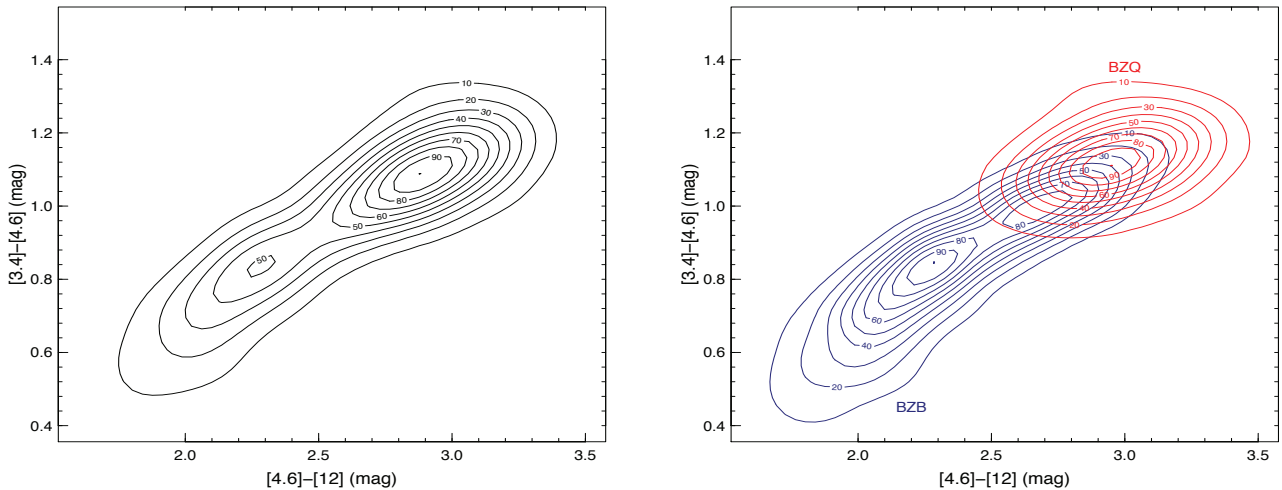


FIG. 1.— Left) The isodensity contours generated by KDE technique in the $[3.4]-[4.6]-[12]$ μm color-color diagram for the whole γ -ray blazar population represented by the sources in the TB sample. Right) The KDE isodensity contours built separately for the BZB (blue) and the BZQ (red) classes in the TB sample. The numbers appearing close to each contour corresponds to the values of π_{kde} in both panels.

of our previous statistical analyses (see Section 2 and D’Abrusco et al. 2013, for more details).

For each radio source with a *WISE* counterpart we applied our KDE technique selecting the radio sources detected by *WISE* at $3.4\mu\text{m}$, $4.5\mu\text{m}$ and $12\mu\text{m}$ with $\pi_{kde} > 0.10$ being fake γ -ray blazar candidates. Then we repeated the entire procedure 10 times for both the NU and the SU sample to establish the probability of spurious associations. Based on the above procedure, we expect that 4%

and 3% of the γ -ray blazar candidates previously selected for the UGS in the NU and SU samples respectively, could be contaminants.

Finally, we emphasize that these estimates depend on the γ -ray background model, the detection threshold and the flux limit of the 2FGL catalog (Nolan et al. 2012), in which no γ -ray emission is arising from any of the positions listed in the fake γ -ray catalogs.

4.3. Comparison with previous investigations

We compare our results with those of previous analyses carried out in Massaro et al. (2013a), Massaro et al. (2013b) and Paggi et al. (2013). The results of our comparison is summarized below and presented in Table 2 and Table 3.

We note that within the 41 γ -ray blazar candidates found in the NU sample there are 16 sources that were also selected on the basis of their three *WISE* colors in Massaro et al. (2013a) 7 that appeared as potential counterpart in Massaro et al. (2013b) found with the low-frequency radio observations and 14 listed with an X-ray properties in Paggi et al. (2013). In addition, 12 UGS were also investigated in our previous analyses but for them we found a different γ -ray blazar candidate. The number of new candidates counterparts in the NU sample is 5. On the other hand, within the SU sample, we found that 8 radio sources were also selected in Massaro et al. (2013a) and 4 in Paggi et al. (2013), in addition to 4 new γ -ray blazar candidates.

Petrov et al. (2013) already found the *WISE* counterparts of their SDA sample but they did not verified which have IR colors consistent with the *Fermi* blazars. Thus in the SDA sample we listed 11 radio sources detected thanks to the deeper radio survey performed with ATCA (Petrov et al. 2013) with IR colors consistent with those of the γ -ray blazar population. Among these 11 γ -ray blazar candidates, there are two sources already found in Massaro et al. (2013a) and only one

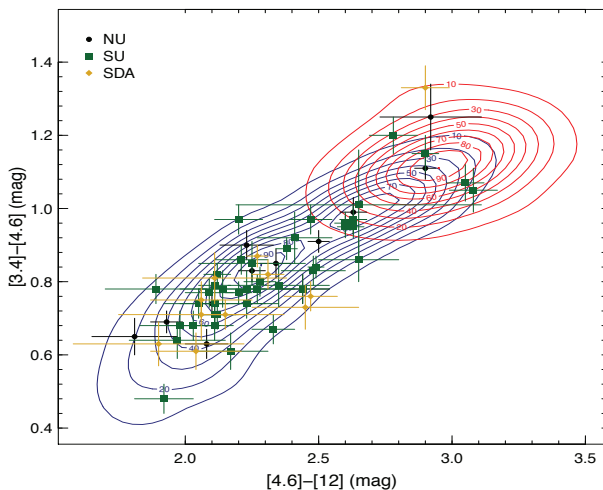


FIG. 2.— The isodensity contours generated by KDE technique in the $[3.4]-[4.6]-[12]$ μm color-color diagram for the BZBs (blue) and the BZQs (red) in the TB sample. Points overlaid to the contours show the location of the selected radio candidates with IR colors consistent with the γ -ray blazar population within $\pi_{kde} > 10$ for the sources in the three different samples analyzed: NU (black circles), SU (green squares) and SDA (yellow diamonds). The numbers appearing close to each contour corresponds to the values of π_{kde} .

TABLE 2
UNIDENTIFIED GAMMA-RAY SOURCES IN THE NORTHERN AND IN THE SOUTHERN SAMPLES.

2FGL name	WISE name	Radio name	[3.4]-[4.6] mag	[4.6]-[12] mag	π_{kde}	notes	z	compare
NORTHERN UGS SAMPLE								
2FGLJ0031.0+0724	J003119.70+072453.6	NVSSJ003119+072456	0.83(0.04)	2.48(0.12)	29.3	N	?	3
2FGLJ0039.1+4331	J003908.14+433014.6	NVSSJ003907+433015	0.97(0.04)	2.20(0.09)	10.3	N,v	?	1,2,3
2FGLJ0103.8+1324	J010345.73+132345.4	NVSSJ010345+132346	0.68(0.04)	2.03(0.10)	31.3	N,M	?	3
2FGLJ0158.4+0107	J015852.76+010132.9	NVSSJ015852+010133	0.85(0.06)	2.25(0.20)	49.1	N,F,s,rv	?	-
2FGLJ0158.6+8558	J015248.80+855703.6	NVSSJ015248+855706	1.07(0.05)	3.05(0.07)	65.6	N,M	?	1,2
2FGLJ0227.7+2249	J022744.35+224834.3	NVSSJ022744+224834	0.95(0.03)	2.60(0.03)	53.1	N,v	?	11,3!
2FGLJ0312.8+2013	J031240.54+201142.8	NVSSJ031240+201141	0.79(0.06)	2.35(0.19)	36.4	N	?	-
2FGLJ0332.1+6309	J033153.90+630814.1	NVSSJ033153+630814	0.96(0.03)	2.60(0.04)	54.5	N,M	?	11,2!
2FGLJ0353.2+5653	J035309.54+565430.8	NVSSJ035309+565431	0.78(0.04)	1.89(0.19)	10.9	N,M,rv	?	21,3!
2FGLJ0409.8-0357	J040946.57-040003.4	NVSSJ040946-040003	0.89(0.03)	2.38(0.04)	46.4	N,M	?	11,3!
2FGLJ0420.9-3743	J042025.09-374445.0	NVSSJ042025-374443	0.78(0.04)	2.44(0.10)	20.2	N,S	?	3!
2FGLJ0600.9+3839	J060102.86+383829.2	NVSSJ060102+383828	0.97(0.04)	2.47(0.08)	38.3	N	?	21,3!
2FGLJ0644.6+6034	J064435.72+603851.2	NVSSJ064435+603849	0.64(0.05)	1.97(0.18)	24.6	N	?	1,21,3
2FGLJ0658.4+0633	J065845.02+063711.5	NVSSJ065844+063711	0.68(0.04)	1.98(0.15)	27.4	N	?	3
2FGLJ0723.9+2901	J072354.83+285929.9	NVSSJ072354+285930	1.15(0.05)	2.90(0.05)	81.0	N,F	?	11,2!,3!
2FGLJ0746.0-0222	J074627.03-022549.3	NVSSJ074627-022549	0.68(0.04)	2.11(0.07)	31.3	N,M	?	11,3!
2FGLJ0928.8-3530	J092849.83-352948.9	NVSSJ092849-352947	0.97(0.04)	2.63(0.05)	57.8	N,S,M	?	-
2FGLJ1016.1+5600	J101544.44+555100.7	NVSSJ101544+555100	1.05(0.06)	3.08(0.09)	48.0	N,F,s	?	11,2!
2FGLJ1115.0-0701	J111511.74-070239.9	NVSSJ111511-070238	0.86(0.06)	2.65(0.15)	17.2	N	?	3
2FGLJ1123.3-2527	J112325.38-252857.0	NVSSJ112325-252858	0.84(0.03)	2.49(0.03)	30.0	N,M,6,QSR	0.146	-
2FGLJ1129.5+3758	J112903.25+375657.4	NVSSJ112903+375655	0.92(0.07)	2.41(0.14)	42.3	N,F,M,s,BL?	?	3
2FGLJ1223.3+7954	J122358.17+795327.8	NVSSJ122358+795329	0.48(0.04)	1.92(0.11)	9.6	N,M	?	21,3
2FGLJ1254.2-2203	J125422.47-220413.6	NVSSJ125422-220413	0.67(0.04)	2.33(0.08)	11.4	N,M,v	?	11,3!
2FGLJ1259.8-3749	J125949.80-374858.1	NVSSJ125949-374856	0.71(0.04)	2.11(0.08)	36.8	N,S,M,v	?	11,3!
2FGLJ1340.5-0412	J134042.02-041006.8	NVSSJ134042-041006	0.71(0.04)	2.12(0.08)	36.6	N,M,v	?	1!
2FGLJ1347.0-2956	J134706.89-295842.3	NVSSJ134706-295840	0.79(0.03)	2.11(0.06)	39.8	N,S,M,v	?	11,3!
2FGLJ1513.5-2546	J151303.66-253925.9	NVSSJ151303-253924	1.01(0.15)	2.65(0.46)	65.9	N	?	3
2FGLJ1517.2+3645	J151649.26+365022.9	NVSSJ151649+365023	0.95(0.03)	2.63(0.04)	54.5	N,F,s,v	?	11,2,3
2FGLJ1548.3+1453	J154824.39+145702.8	NVSSJ154824+145702	0.74(0.05)	2.11(0.19)	39.6	N,F,M,s	?	-
2FGLJ1647.0+4351	J164619.95+435631.0	NVSSJ164619+435631	0.77(0.04)	2.09(0.09)	38.1	N,F,s,X	?	1!
2FGLJ1704.3+1235	J170409.59+123421.7	NVSSJ170409+123421	0.74(0.04)	2.05(0.07)	35.4	N,M	?	3
2FGLJ1704.6-0529	J170433.84-052840.6	NVSSJ170433-052839	0.78(0.05)	2.14(0.16)	43.0	N,M,v	?	3
2FGLJ2004.6+7004	J200506.02+700439.3	NVSSJ200506+700440	0.77(0.03)	2.20(0.05)	45.7	N,v	?	11,3
2FGLJ2021.5+0632	J202155.45+062913.7	NVSSJ202155+062914	0.82(0.03)	2.12(0.05)	35.3	N,M	?	11,3!
2FGLJ2115.4+1213	J211522.00+121802.8	NVSSJ211522+121802	0.78(0.05)	2.23(0.18)	46.2	N,M	?	3!
2FGLJ2132.5+2605	J213253.05+261143.8	NVSSJ213252+261143	1.20(0.05)	2.78(0.09)	25.9	N	?	3
2FGLJ2133.9+6645	J213349.21+664704.3	NVSSJ213349+664706	0.80(0.04)	2.28(0.06)	49.0	N,v	?	11,2,3
2FGLJ2134.6-2130	J213430.18-213032.6	NVSSJ213430-213032	0.78(0.04)	2.27(0.08)	44.3	N,M	?	11,3
2FGLJ2228.6-1633	J222830.19-163642.8	NVSSJ222830-163643	0.74(0.04)	2.23(0.12)	37.9	N,M	?	3!
2FGLJ2246.3+1549	J224604.98+154435.3	NVSSJ224604+154437	0.61(0.05)	2.17(0.14)	16.0	N,M	?	3!
2FGLJ2358.4-1811	J235836.83-180717.3	NVSSJ235836-180718	0.86(0.04)	2.21(0.10)	43.2	N,M,6,X,BL	0.058?	1
SOUTHERN UGS SAMPLE								
2FGLJ0116.6-6153	J011619.59-615343.5	SUMSSJ011619-615343	0.85(0.04)	2.34(0.06)	49.9	S,M	?	11,3!
2FGLJ0133.4-4408	J013306.35-441421.3	SUMSSJ013306-441422	0.83(0.03)	2.25(0.05)	51.0	S,M	?	11,3!
2FGLJ0143.6-5844	J014347.39-584551.3	SUMSSJ014347-584550	0.69(0.03)	1.93(0.06)	23.0	S,M	?	11,3
2FGLJ0316.1-6434	J031614.31-643731.4	SUMSSJ031614-643732	0.74(0.03)	2.10(0.06)	38.9	S,M	?	11,3
2FGLJ0416.0-4355	J041605.81-435514.6	SUMSSJ041605-435516	1.11(0.03)	2.90(0.04)	97.2	S,M	?	1!
2FGLJ0420.9-3743	J042025.09-374445.0	MRSS303-096250	0.78(0.04)	2.44(0.10)	20.2	N,S	?	3!
2FGLJ0555.9-4348	J055618.74-435146.1	SUMSSJ055618-435146	0.91(0.03)	2.50(0.04)	43.9	S,M	?	1!
2FGLJ0928.8-3530	J092849.83-352948.9	SUMSSJ092849-352947	0.97(0.04)	2.63(0.05)	57.8	N,S,M	?	-
2FGLJ1032.9-8401	J103015.35-840308.7	SUMSSJ103014-840307	0.99(0.04)	2.63(0.05)	62.1	S,v	?	1!
2FGLJ1259.8-3749	J125949.80-374858.1	SUMSSJ125949-374856	0.71(0.04)	2.11(0.08)	36.8	N,S,M,v	?	11,3!
2FGLJ1328.5-4728	J132840.61-472749.2	SUMSSJ132840-472748	0.63(0.04)	2.08(0.08)	24.4	S,M,v	?	3!
2FGLJ2042.8-7317	J204201.92-731913.5	SUMSSJ204201-731911	0.65(0.05)	1.81(0.16)	12.1	S,M	?	-
2FGLJ2131.0-5417	J213208.28-542036.4	SUMSSJ213208-542037	1.25(0.09)	2.92(0.19)	29.0	S	?	-
2FGLJ2213.7-4754	J221330.33-475425.0	SUMSSJ221330-475426	0.90(0.04)	2.23(0.10)	33.4	S,M	?	-

Col. (1) 2FGL name.
 Col. (2) WISE name.
 Col. (3) Radio name.
 Cols. (4,5) IR colors from WISE. Values in parentheses are 1σ uncertainties.
 Col. (6) Notes: N = NVSS, F = FIRST, M = 2MASS, s = SDSS dr9, 6 = 6dFG; X=ROSAT; QSO = quasar, BL = BL Lac; v = variable in WISE bands (var_flag > 5 in at least one band, see Cutri et al. 2012 for additional details); rv = variable in the radio bands at 1.4 GHz.
 Col. (7) Estimate level of confidence derived from the KDE analysis.
 Col. (8) Redshift: ? = unknown.
 Col. (9) Results of the comparison with previous analyses. 1 = UGS analyzed in Massaro et al. (2013a), 2 = UGS analyzed in Massaro et al. (2013b) 3 = UGS analyzed in Paggi et al. (2013). Exclamation mark (!) indicates that the γ -ray blazar candidate is the same IR source found in the previous investigation.

363 UGS (i.e., 2FGLJ0547.5-0141c) previously investigated
 364 that appear to have a different potential counterpart.
 365 We note that the comparison between the γ -ray blazar
 366 candidates found in the SU and in the SDA samples
 367 and those presented in Massaro et al. (2013b) based
 368 on the WENSS radio analysis was not possible because
 369 the footprints of the surveys used did not overlap. We
 370 also verified that the selected γ -ray blazar candidates
 371 having a SDSS counterpart exhibit optical color con-
 372 sistent with those of BL Lacs (i.e., $u - r < 1.4$, see
 373 Massaro et al. 2012, for more details). We found that
 374 with the only exception of NVSSJ154824+145702 all of
 375 them have the same optical properties of the BZB pop-
 376 ulation.
 377 Within the whole sample of UGSs analyzed, there are
 378 25 sources that were also unidentified in the 1FGL (?)
 379 and were analyzed on the basis of two different statisti-
 380 cal approaches: the Classification Tree and the Logistic
 381 regression analyses (see Ackermann et al. 2012, and ref-
 382 erences therein). By comparing the results of our asso-
 383 ciation method with those in Ackermann et al. (2012),
 384 we found that 19 out of 25 UGSs with a γ -ray blazar
 385

TABLE 3
UNIDENTIFIED GAMMA-RAY SOURCES IN THE SDA SAMPLE.

2FGL name	WISE name	IAU name	[3.4]-[4.6] mag	[4.6]-[12] mag	π_{kde}	notes	z	compare
2FGLJ0200.4-4105	J020020.94-410935.6	J0200-4109	0.63(0.06)	1.90(0.32)	19.3	6,X	?	
2FGLJ0340.7-2421	J034022.89-242407.2	J0340-2424	0.73(0.06)	2.45(0.20)	10.0	N	?	
2FGLJ0523.3-2530	J052313.07-253154.4	J0523-2531	1.33(0.06)	2.90(0.09)	9.5	-	?	
2FGLJ0547.5-0141c	J054720.85-013329.9	J0547-0133	0.81(0.07)	2.11(0.27)	36.6	N	?	1
2FGLJ0937.9-1434	J093754.72-143350.3	J0937-1433	0.71(0.04)	2.15(0.08)	35.1	N	?	
2FGLJ1315.6-0730	J131552.98-073301.9	J1315-0733	0.87(0.03)	2.27(0.04)	47.2	N,F,M,v,BL?	?	!!
2FGLJ1339.2-2348	J133916.44-234829.4	J1339-2348	0.75(0.05)	2.06(0.19)	35.0	N	?	
2FGLJ1345.8-3356	J134543.05-335643.3	J1345-3356	0.82(0.04)	2.31(0.06)	49.8	N,S,M	?	!!
2FGLJ2034.7-4201	J203451.08-420038.2	J2034-4200	0.61(0.05)	2.04(0.17)	22.3	-	?	
2FGLJ2251.1-4927	J225128.69-492910.6	J2251-4929	0.76(0.04)	2.47(0.10)	12.1	S	?	
2FGLJ2343.3-4752	J234302.29-475749.9	J2343-4757	0.71(0.07)	2.06(0.31)	35.4	S	?	

Col. (1) 2FGL name.

Col. (2) WISE name.

Col. (3) Radio name.

Cols. (4,5) IR colors from *WISE*. Values in parentheses are 1σ uncertainties.

Col. (6) Notes: N = NVSS, F = FIRST, M = 2MASS, s = SDSS dr9, 6 = 6dFG; X=ROSAT; QSO = quasar, BL = BL Lac; v = variable in *WISE* bands ($\text{var_flag} > 5$ in at least one band, see Cutri et al. 2012 for additional details); rv = variable in the radio bands at 1.4 GHz.

Col. (7) Estimate level of confidence derived from the KDE analysis.

Col. (8) Redshift: ? = unknown.

Col. (9) Results of the comparison with previous analyses. 1 = UGS analyzed in Massaro et al. (2013a), 2 = UGS analyzed in Massaro et al. (2013b) 3 = UGS analyzed in Paggi et al. (2013). Exclamation mark (!) indicates that the γ -ray blazar candidate is the same IR source found in the previous investigation.

386 candidate recognized according to our method are also
387 classified as AGNs. All of them with a probability higher
388 than 60% with 14 higher than 80%. The remaining three
389 sources were classified as pulsar candidates but with a
390 very low probability (i.e. $\leq 60\%$) Consequently, our re-
391 sults are in good agreement with the classification sug-
392 gested previously by Ackermann et al. (2012) and thus
393 consistent with the γ -ray AGN nature.

394 Finally, we remark that several γ -ray pulsars have been
395 identified after the release of the 2FGL, where they are
396 listed as UGSs. However, we did not exclude these UGSs
397 from our sample to test if, as expected, we did not find
398 any blazar-like counterpart associable to them. Thus,
399 in agreement with our expectations, all the UGSs for
400 which we found a γ -ray blazar candidates do not have
401 any pulsars associated according to the Public List of
402 LAT-Detected Gamma-Ray Pulsars⁹.

403 5. SUMMARY AND CONCLUSIONS

404 In this paper we presented a non-parametric method
405 to search for γ -ray blazar candidates within two sam-
406 ples of UGSs. First we identify all the radio
407 sources in the two major surveys (i.e., NVSS and
408 SUMSS Condon et al. 1998; Mauch et al. 2003, respec-
409 tively) that lie within the positional uncertainty re-
410 gion at 95% level of confidence, then we investigate
411 the IR colors of their *WISE* counterparts to recognize
412 those with similar spectral properties in the simple [3.4]-
413 [4.6]-[12] color-color plot. With respect to our previ-
414 ous *WISE* selection of γ -ray blazar candidates (e.g.,
415 Massaro et al. 2012a; D’Abrusco et al. 2013) the crite-
416 ria adopted in the present analysis are less conservative,
417 since the detection of the *WISE* counterpart at $22\mu\text{m}$
418 is not required. A small fraction ($\sim 8\%$) of the *Fermi*
419 blazar are in fact not detected at $22\mu\text{m}$. Thus, to com-
420 pare the IR colors of the *Fermi* blazars with those of the
421 radio sources selected, we adopted a KDE technique as
422 already presented in Massaro et al. (2011a), Massaro et
423 al. (2012a) and more recently in Paggi et al. (2013). Our
424 new approach, being less restrictive than those adopted
425 in our previous associations, permits to search for faint
426 γ -ray blazar candidates that were not previously selected
427 because too faint at $22\mu\text{m}$. By relaxing the requirement

428 on the detection at $22\mu\text{m}$ and thus on the [12]-[22] color,
429 this method would select candidate blazars at the cost of
430 a larger contamination, mitigated by the requirement on
431 the presence of a radio counterpart.

432 We found 41 and 14 radio sources with IR similar
433 to those of the *Fermi* blazars within the NU and the
434 SU samples, respectively. In addition, we investigated
435 the sample of radio sources discovered with recent deep
436 ATCA observations performed to search for radio coun-
437 terparts of the UGS in the southern hemisphere. Among
438 416 radio objects listed in Petrov et al. (2013) only 11
439 sources have an IR counterpart consistent with the γ -ray
440 blazars. The total number of γ -ray blazar candidates is
441 66 all listed in Table 2 and Table 3. without no multi-
442 ple candidates within the positional uncertainty regions
443 of the UGSs analyzed. **We estimate a probability**
444 **of spurious association for the γ -ray blazar candi-**
445 **dates selected according to our method of the**
446 **order of 4% and 3% for the NU and SU samples,**
447 **respectively.**

448 It is worth noting that the large majority of our candi-
449 dates show IR colors more consistent with the region oc-
450 cupied by the BZBs in the [3.4]-[4.6]-[12] μm color-color
451 diagram rather than that of BZQs. Thus they could be
452 potential faint and so distant BZBs that were not previ-
453 ously selected with different methods because lacking of
454 the IR flux at $22\mu\text{m}$. More detailed investigations based
455 on ground-based, optical and near IR, spectroscopic fol-
456 low up observations will be planned for the selected γ -ray
457 blazar candidates to confirm their nature and to obtain
458 their redshifts.

460 The work is supported by the NASA grants
461 NNX12AO97G. R. D’Abrusco gratefully acknowledges
462 the financial support of the US Virtual Astronomical
463 Observatory, which is sponsored by the National Sci-
464 ence Foundation and the National Aeronautics and Space
465 Administration. The work by G. Tosti is supported by
466 the ASI/INAF contract I/005/12/0. Howard A. Smith
467 acknowledges partial support from NASA-JPLRSA con-
468 tract 717437. TOPCAT¹⁰ (Taylor 2005) for the prepa-
469 ration and manipulation of the tabular data and the

⁹ <https://confluence.slac.stanford.edu/display/GLAMCOG/Public+List+of+LAT+Detected+Gamma+Ray+Pulsars>

TABLE 4
OPTICAL MAGNITUDES FOR THE *WISE* COUNTERPARTS.

WISE name	B1 mag	R1 mag	B2 mag	R2 mag	I mag	θ arcsec
J003119.70+072453.6	19.03	18.17	19.84	18.63	18.67	0.14
J003908.14+433014.6	19.9	19.61	21.42	20.77		0.14
J010345.73+132345.4	17.98	17.73	18.69	17.38	17.24	0.07
J011619.59-615343.5		17.72	18.22	17.78	17.91	0.27
J013306.35-441421.3		18.38	19.7	18.12	18.76	0.26
J014347.39-584551.3		16.7	18.48	16.64	17.04	0.04
J015248.80+855703.6	20.57	18.84	19.63	18.71	17.82	0.38
J020020.94-410935.6		19.84	21.1	18.79	18.75	0.6
J022744.35+224834.3			20.82	20.22	19.28	0.35
J031240.54+201142.8		19.34	21.22	19.42	19.07	2.63
J031614.31-643731.4		16.59	18.19	16.57	16.82	0.22
J033153.90+630814.1			20.66	19.92	18.35	0.35
J034022.89-242407.2		19.56	20.07			0.21
J035309.54+565430.8	20.09	19.24	20.43	18.76	18.53	0.55
J040946.57-040003.4	19.45	19.18	17.53	16.98	16.86	0.07
J041605.81-435514.6		18.49	18.7	18.17	18.0	0.18
J042025.09-374445.0		20.44	20.73	19.71	18.17	0.38
J052313.07-253154.4		19.2	20.83	20.07	18.95	0.17
J055618.74-435146.1		19.23	18.88	19.08	18.08	0.31
J060102.86+383829.2		19.11		19.84	18.48	0.04
J064435.72+603851.2	20.01	19.58	20.7	18.75	18.37	0.3
J065845.02+063711.5	20.25			19.12	18.3	0.39
J072354.83+285929.9	19.78	19.05	19.97	18.72		0.19
J074627.03-022549.3	19.03		18.59	18.43	16.53	0.31
J092849.83-352948.9		18.56	19.64	18.07	18.23	0.23
J093754.72-143350.3	18.82	17.92	18.64	17.73	17.56	0.1
J101544.44+555100.7	19.69	19.42	20.61	19.35		0.37
J103015.35-840308.7		19.36	19.26	18.84	18.03	0.15
J111151.74-070239.9		19.86	20.68	19.05	18.66	0.14
J112325.38-252857.0	16.9	15.76	15.87	15.56	15.51	0.19
J112903.25+375657.4	19.9	19.23	19.35	19.48	18.58	0.65
J122358.17+795327.8		17.6	20.18	18.46	17.63	1.04
J125422.47-220413.6		19.88	18.67	19.11	18.22	0.41
J125949.80-374858.1		17.44	18.07	16.78	17.35	0.17
J131552.98-073301.9	19.78	18.68	18.75	17.75	17.56	0.16
J132840.61-472749.2		17.75	18.23	16.8		0.98
J133916.44-234829.4	20.3	19.3	20.43	19.79	18.5	0.31
J134042.02-041006.8	18.21	17.21	17.59	16.46	17.08	0.19
J134543.05-335643.3		17.98	19.58	18.65	18.12	0.38
J134706.89-295842.3	17.85	17.09	18.8	17.14	17.09	0.41
J151303.66-253925.9	19.92	18.96	19.77	20.35		0.5
J151649.26+365022.9	20.9		21.49	20.07	19.16	1.58
J154824.39+145702.8	20.51	18.29	19.86	17.74	17.45	0.41
J164619.95+435631.0	20.43	19.73	20.42	19.67		0.34
J170409.59+123421.7	19.86	18.04	18.62	17.63	17.46	0.47
J170433.84-052840.6	19.62	18.97	18.42	17.28	17.98	0.45
J200506.02+700439.3	20.73	19.25	19.24	18.65		0.45
J202155.45+062913.7	17.27	16.13	17.01	16.67	16.03	0.43
J203451.08-420038.2		18.97	19.34	18.87	18.27	0.44
J204201.92-731913.5		17.46	17.9	18.36	18.04	0.29
J211522.00+121802.8	18.15	18.15	17.68	17.31	17.58	0.16
J213253.05+261143.8	20.04	19.29	19.14	19.62	18.44	0.07
J213430.18-213032.6	19.77	18.65	18.96	16.8	17.7	0.09
J213349.21+664704.3				19.37	18.8	0.45
J221330.33-475425.0		18.12	18.6	18.34	18.33	0.05
J222830.19-163642.8	18.57	19.34	19.95	19.04	17.91	0.29
J224604.98+154435.3	19.14	18.27	19.57	18.53	17.65	0.13
J225128.69-492910.6		18.8	19.21	18.45	18.03	0.42
J234302.29-475749.9		19.84	18.92	21.3	18.32	0.29
J235836.83-180717.3	19.14	18.45	18.28	17.22	17.53	0.3

470 images. The WENSS project was a collaboration be-
471 tween the Netherlands Foundation for Research in As-
472 tronomy and the Leiden Observatory. We acknowledge
473 the WENSS team consisted of Ger de Bruyn, Yuan
474 Tang, Roeland Rengelink, George Miley, Huub Rottger-
475 ing, Malcolm Bremer, Martin Bremer, Wim Brouw,
476 Ernst Raimond and David Fullagar for the extensive
477 work aimed at producing the WENSS catalog. Part of
478 this work is based on archival data, software or on-line
479 services provided by the ASI Science Data Center. This
480 research has made use of data obtained from the High
481 Energy Astrophysics Science Archive Research Center
482 (HEASARC) provided by NASA's Goddard Space Flight
483 Center; the SIMBAD database operated at CDS, Stras-
484 bourg, France; the NASA/IPAC Extragalactic Database
485 (NED) operated by the Jet Propulsion Laboratory, Cal-
486 ifornia Institute of Technology, under contract with the
487 National Aeronautics and Space Administration. Part
488 of this work is based on the NVSS (NRAO VLA Sky
489 Survey); The National Radio Astronomy Observatory is
490 operated by Associated Universities, Inc., under contract
491 with the National Science Foundation. This publication
492 makes use of data products from the Two Micron All
493 Sky Survey, which is a joint project of the University of
494 Massachusetts and the Infrared Processing and Analysis
495 Center/California Institute of Technology, funded by the
496 National Aeronautics and Space Administration and the
497 National Science Foundation. This publication makes
498 use of data products from the Wide-field Infrared Sur-
499 vey Explorer, which is a joint project of the University
500 of California, Los Angeles, and the Jet Propulsion Labo-
501 ratory/California Institute of Technology, funded by the
502 National Aeronautics and Space Administration.

503

REFERENCES

- 504 Abdo, A. A. et al. 2010a ApJS 188 405
505 Abdo, A. A. et al. 2010b ApJ, 720, 435
506 Ackermann, M. et al. 2011b ApJ, 743, 171
507 Ackermann, M. et al. 2011a ApJ, 741, 30
508 Ackermann, M. et al. 2012 ApJ, 753, 83
509 Adelman-McCarthy, J., Agueros, M.A., Allam, S.S., et al. 2008,
510 ApJS, 175, 297
511 Becker, R. H., White, R. L., Helfand, D. J. 1995 ApJ, 450, 559
512 Condon, J. J., Cotton, W. D., Greisen, E. W., Yin, Q. F., Perley,
513 R. A., Taylor, G. B., & Broderick, J. J. 1998, AJ, 115, 1693
514 Cutri et al. 2012 wise.rept, 1C
515 D'Abrusco, R., Longo, G., Walton, N. A. 2009 MNRAS, 396, 223
516 D'Abrusco, R., Massaro, F., Ajello, M., Grindlay, J. E., Smith,
517 Howard A. & Tosti, G. 2012 ApJ, 748, 68
518 D'Abrusco, R., Massaro, F., Paggi, A., Masetti, N., Giroletti, M.,
519 Tosti, G., Smith, Howard, A. 2013 ApJS, 206, 12
520 Draine B. T. 2003 ARA&A, 41, 241
521 Ghirlanda, G., Ghisellini, G., Tavecchio, F., Foschini, L. 2010
522 MNRAS, 407, 791
523 Hartman, R.C. et al., 1999 ApJS, 123, 79
524 Kovalev, Y. Y. 2009 ApJ, 707L, 56
525 Kovalev, Y. Y. et al. 2009 ApJ, 696L, 17
526 Jones, H. D. et al. 2004 MNRAS, 355, 747
527 Jones, H. D. et al. 2009 MNRAS, 399, 683
528 Laurino, O. & D'Abrusco 2011 MNRAS in press
529 Mahony, E. K., Sadler, E. M., Murphy, T., Ekers, R. D.,
530 Edwards, P. G., Massardi, M. 2010 ApJ, 718, 587
531 Massaro, E., Giommi, P., Leto, C., Marchegiani, P., Maselli, A.,
532 Perri, M., Piranomonte, S., Scavi, S. 2009 A&A, 495, 691
533 Massaro, E., Giommi, P., Leto, C., Marchegiani, P., Maselli, A.,
534 Perri, M., Piranomonte, S., Scavi, S. 2010
535 <http://arxiv.org/abs/1006.0922>

- 536 Massaro, F., D'Abrusco, R., Ajello, M., Grindlay, J. E. & Smith,
537 H. A. 2011a ApJ, 740L, 48
- 538 Massaro, E., Giommi, P., Leto, C., Marchegiani, P., Maselli, A.,
539 Perri, M., Piranomonte, S., 2011b "Multifrequency Catalogue
540 of Blazars (3rd Edition)", ARACNE Editrice, Rome, Italy
- 541 Massaro, F., D'Abrusco, R., Tosti, G., Ajello, M., Gasparrini, D.,
542 Grindlay, J. E. & Smith, Howard A. 2012a ApJ, 750, 138
- 543 Massaro, F., D'Abrusco, R., Tosti, G., Ajello, M., Paggi, A.,
544 Gasparrini, D. 2012b ApJ, 752, 61
- 545 Massaro, E., Nesci, R., Piranomonte, S. 2012 MNRAS ,422, 2322
- 546 Massaro, F. et al. 2013a ApJS, 206, 13
- 547 Massaro, F. et al. 2013b ApJS, 207, 4
- 548 Mauch, T., Murphy, T., Buttery, H. J., Curran, J., Hunstead, R.
549 W., Piestrzynski, B., Robertson, J. G., Sadler, E. M. 2003
550 MNRAS, 342, 1117
- 551 Mirabal, N. 2009 [arxiv.org/abs/0908.1389v2]
- 552 Mirabal, N. 2009 ApJ, 701, 129
- 553 Mirabal, N, D. & Pardo, S. 2010 A&A submitted,
554 [arxiv.org/abs/1007.2644v2]
- 555 Monet, D. G. et al. 2003 AJ, 125, 984
- 556 Mukherjee, R. et al., 1997 ApJ, 490, 116
- 557 Nolan et al. 2012 ApJS, 199, 31
- 558 Petrov, L., Mahony, E. K., Edwards, P. G., Sadler, E. M.,
559 Schinzel, F. K., McConnell, D. 2013 MNRAS, 432, 1294
- 560 Paggi, A., Massaro, F., D'Abrusco, R. et al. 2013 ApJS submitted
- 561 Paris, I. et al. 2012 A&A, 548A, 66
- 562 Rengelink, R. et al. 1997, A&A Suppl. 124, 259
- 563 Richards, G. T. et al., 2004 ApJS, 155, 257
- 564 Skrutskie, M. F. et al. 2006, AJ, 131, 1163
- 565 Takeuchi Y. et al., 2013, ApJS submitted
- 566 Taylor M. B., 2005, ASPC, 347, 29
- 567 Thompson, D. J. 2008 RPPh, 71, 11, 116901
- 568 Ungruhe, R., Seitter, W. C., Duerbeck, H. W. 2003 JAD, 9, 1
- 569 Voges, W. et al. 1999 A&A, 349, 389
- 570 White, R. L., Becker, R. H. Helfand, D. J., Gregg, M. D. et al.
571 1997 ApJ, 475, 479
- 572 Wright, E. L., et al. 2010 AJ, 140, 1868
- 573 Zechlin, H.-S., Fernandes, M. V., Elsasser, D., Horns, D. 2012
574 A&A, 538A, 93